

MICROSTRUCTURE ANALYSIS IN MICROSCOPIC IMAGES FOR CLASSIFICATION OF STEEL ALLOYS USING DEEP NEURAL ARCHITECTURES

Mrs.K.Andal

Research Scholar, Department of Computer Science and Engineering, Annamalai University
sanandal86@gmail.com

Mrs.S.Sathiya

Assistant Professor, Department of Computer Science and Engineering, Annamalai
University
Sathiya.sep05@gmail.com

Mr.P.Sivaraj

Associate Professor, Department of Manufacturing Engineering, Annamalai University
cemajorsiva@gmail.com

ABSTRACT

Microstructure refers to a material's internal structure. It records a material's origin and establishes all of its chemical and physical attributes. Although microstructural characterization is common and well-known, microstructural classification is typically carried out manually by human experts, which introduces subjectivity-related uncertainties. Only a few previous studies exist since it is extremely difficult to automatically classify microstructures because they may be a combination of various phases or constituents with complicated substructures. Previous studies concentrated on expertly created and constructed features and separated the classification of microstructures from the feature extraction stage. By simultaneously learning the features from the input and the classification phase, Deep Learning techniques have recently demonstrated outstanding performance in vision applications. In this work, it is suggested to apply a Deep Learning algorithm to classify low carbon steel's microstructure using instances of certain microstructural elements. This work proposes the classification of the steel alloys based on the features of microstructure, which were extracted through an External Attention Transformer network (EATNet). Combining the external attention mechanism with the transformer can provide better performance when compared to conventional Convolutional Neural Network based approach. The proposed classification models were trained using microstructure images of ferritic-martensitic steels containing 9 to 12 wt% Cr, also referred to as 9% Cr steel.

Keywords: *microstructural classification, Deep Learning techniques, External Attention Transformer network, conventional Convolutional Neural Network, ferritic-martensitic steels*

INTRODUCTION

In the last 40 years, big forgings and castings of steam power plants, as well as thick-section components like pipelines, have found growing use of martensitic creep resistant 9–12% Cr steels. The four pillars of materials research are composition, processing, microstructure, and

material properties. [1] The main methods for characterizing materials and providing the foundation for describing material behavior are optical microscopy, scanning electron microscopy (SEM), and transmission electron microscopy, to name three. Microstructures at different length scales can be acquired by various techniques. Understanding of the microstructure stability of this class of alloys has advanced significantly thanks to new breakthroughs in better microstructure imaging tools and improved microstructure models. Individual researchers often study microstructure photos, and their experience influences how they perceive the microstructure-mechanical behavior. Instead of depending on single-point individual interpretations, artificial intelligence (AI), or more precisely machine learning (ML), [2] has recently become more widely utilized in materials research to acquire and process the microscopic images and under the correlation between microstructure and the mechanical properties [3] or classify the category of alloy. By utilizing contemporary artificial neural networks, this opens up fresh and intriguing study prospects.

Consider the commonly used type of material, 9% Cr martensite/ferrite steels, in which ML approaches are employed to handle the problem of determining composition-microstructure-mechanical property. The 621 SEM digital photomicrographs of 9% Cr steels with various element concentrations (labelled as HR, P92, and CPJ based on element concentrations) serve as the input data for the ML model. When the processing conditions are regulated and kept constant, the microstructure produced by an alloy with the same composition will be the same. Since we have many of these photos for the same alloy, a huge training samples of microstructure images helps reduce the impact of unintentional factors, which is useful for building a successful deep neural architectures which are considered to be data hungry model. The classification process is strengthened using a combination of transformer and attention techniques. According to the significance of activation, the attention technique can be seen as a process for reallocating resources. It is crucial to the functioning of the human visual system. The last ten years have seen rapid advancement in this subject. The research in [4] proposed SENet, demonstrating how the noise-canceling capabilities of the attention mechanism can enhance classification performance.

Self-attention is a specific case of attention. The main principle of self-attention is computing the similarity among features to capture long-range interdependence. However, the computational and storage overheads quadratically rise with the depth of the feature map [31]. The external attention computes the relationship between self-queries and a much smaller learnable key memory, which captures the overall context of the dataset, as opposed to self-attention, which derives an attention map by calculating affinities between self-queries and self-keys. Since external attention doesn't really rely on semantic data, it can be optimized end-to-end by the back-propagation process without the need for an iterative approach. With enough training data, a transformer outperforms a conventional CNN, according to the suggested architecture based on patch encoding and a transformer in [6]. One way to conceptualize self-attention is as a linear combination of self-values that refines the input feature. The requirement for a $N \times N$ self attention matrix and a N element self value matrix in this linear transformation, however, is far from clear. Additionally, self-attention only takes into account the relationships between items inside a data sample and ignores potential relationships between elements in various samples, which may restrict its flexibility and capacity [26][28].

LITERATURE SURVEY

This section presents an overview of various deep learning based solutions proposed in literature for solving problems in the field metal microscopic image analysis. Deep learning has recently accelerated the development of its applications in a variety of fields, including social network analysis[8], information retrieval[9], speech and audio processing[10], visual data processing[11], natural language processing[12], and others. In the area of materials science, deep learning methods have also been tried [13], including structure prediction and design [14], chemistry learning [15], structure-property linkage analysis [16], and structure characterization [17]. Microscopical imaging analysis, which uses objects to obtain the real-space information of materials, is particularly significant among all research topics. Two issues with SEM image analysis have been resolved using deep learning: the first is the classification of microscopic pictures based on their morphological characteristics [18], and the second is resolution improvement to enhance the image quality [19]. The authors of [20] used a pre-trained deep learning network to classify microscopic pictures. The authors demonstrated that Inception-v3 [21], which was constituted of symmetric and asymmetric blocks including convolutions, pooling, concatenations, etc., performed better than others on both accuracy and computational efficiency. The authors analyzed the findings of four different deep learning models (Inception-slim, Inception-v3, Inception-v4 and ResNet)[27].

A pixel-by-pixel categorization on photographs of carbon steel is an additional example [18]. The process of classifying an image pixel-by-pixel has the advantage of revealing information about the shape and area of each object, as opposed to the global picture classification used in the example above. An object-based convolutional neural network was suggested in the work of [22] for classifying elements and phases. For pixel-wise segmentation on low carbon-steel SEM or Light Optical Microscopy (LOM) pictures, a network known as max-voted fully convolutional neural networks (FCNN) [MVFCNN] was developed. Identification and classification of the structural and rotational states of surface molecules are additional applications [23]. The framework was able to determine if each molecule was in the bowl-up or bowl-down condition and classify the rotation into four groups by fusing the Markov network and convolutional neural network[32-38]. This paper shall work on developing solutions to enhance the performance of the CNN model by including a combination of attention mechanism and transformer technique. Spatial attention enables neural networks to learn the locations that should be the focus of attention[30]. The important information is kept while the spatial information from the original image is changed into another space through this attention process[29].

MATERIALS AND METHOD

Dataset

Scanning Electron Microscope digital photomicrographs of 9% Cr martensite/ferrite steels with various concentrations are considered in this study for training the classification model. When the processing conditions are regulated and kept constant, the microstructure produced by an alloy with the same composition will be the same. However, some environmental noises may have an impact on the actual alloy synthesis process, adding some uncertainty. Images of three different steel alloys, P92, HR, and CPJ, are available in this dataset. First, the images are cleaned by removing any unnecessary components, including the labels for the enhancing information on the images produced by the microscope. In order to classify the images, the

deep neural architecture decreases the spatial dimensionality of the microstructure images and extracts the key information from the images. The Table 1 present the details on the number of data samples used for classification in each category.

Table. 1 Class Distribution

Category	No. of Images
P92	188
HR	244
CPJ	300

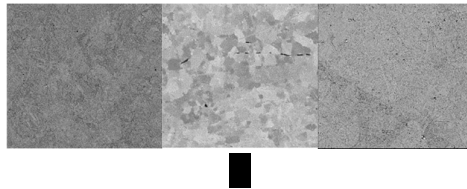


Fig. Sample Image of CPJ, HR, and P92 steel alloys

Normalization

For normalizing the attention map the softmax based normalization is employed so that $\sum_j \alpha_{i,j} = 1$. However, matrix multiplication is used to determine the attention map. The attention map is sensitive to the scale of the input features, in contrast to cosine similarity. The work in [5] uses double normalization, which independently normalizes columns and rows, as suggested in [7], to resolve this issue. The double normalization was formulated as;

$$(\tilde{\alpha})_{i,j} = FM_k^T$$

$$(\tilde{\alpha})_{i,j} = \exp(\tilde{\alpha}_{i,j}) / \sum_k \tilde{\alpha}_{i,k}$$

External Attention Algorithm

Consider a feature map represented as $F \in \mathbb{R}^{N \times d}$ where N is the number of pixels in images and d is the dimension of the feature. The self-attention mechanism projects the input to the following matrices; query matrix - $Q \in \mathbb{R}^{N \times d'}$, key matrix $K \in \mathbb{R}^{N \times d'}$, and value matrix- $V \in \mathbb{R}^{N \times d}$. The self-attention mechanism can be mathematically expressed as follows;

$$A = (\alpha)_{i,j} = \text{softmax}(QK^T)$$

$F_{out} = AV$, where $A \in \mathbb{R}^{N \times N}$ represents the attention matrix, and $\alpha_{i,j}$ presents the similarity between the i^{th} and j^{th} pixel. A variant of self-attention estimates the attention map from the feature F which is represented mathematically as given below;

$$A = \text{softmax}(FF^T)$$

$$F_{out} = AF$$

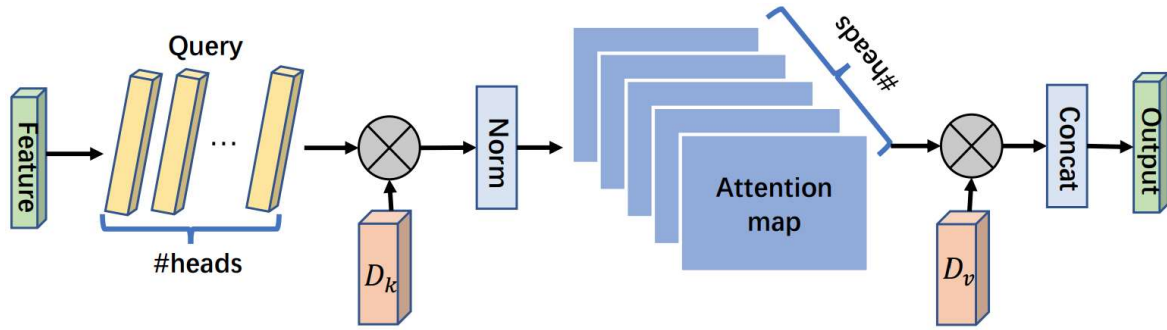


Fig. Schematic view of External-Attention [5]

By calculating pixel-by-pixel resemblance in the feature space, the attention map is created in this case, and the outcome is a more accurate feature description of the input. Self-attention utilization, however, suffers significantly from the enormous computational complexity of $\theta(dN^2)$, even after it has been simplified. Direct application of self-attention to images is not practicable due to the quadratic complexity with respect to the number of input pixels. In order to reduce the computational complexity, earlier work [6] uses self-attention on regions rather than pixels. The external attention estimates the attention input pixels and the external memory unit $M \in \mathbb{R}^{S \times d}$;

$$A = (\alpha)_{i,j} = Norm(FM^T)$$

$$F_{out} = AM.$$

The similarity between the i -th pixel and the j -th row of M , which is a learnable quantity independent of the input and serves as a memory of the entire training dataset, is represented by i,j in Equation (5) as opposed to self-attention. The attention map, A , is normalized similarly to self-attention and is inferred using this learnt dataset-level prior knowledge. Finally, using the similarities in A , we update the input characteristics from M . For increasing the capacity of the network two different memory units M_k and M_v were used as the key and value by which the external attention computation can be expressed as;

$$A = Norm(FM_k^T)$$

$$F_{out} = AM_v$$

This technique is linear in the number of pixels since d and S are hyper-parameters and the computation cost of external attention is $\theta(dSN)$. In reality, it was discovered that trials perform best with a modest value of S as 64. As a result, external attention is far more effective than self-attention and can be used to process large-scale data directly. Additionally, it should be mentioned that the computational cost of external attention is about similar to a convolution of size 1 by 1.

Transformer

Transformer [24], which uses an attention-based structure, has first shown how much of an impact it has on the machine translation and sequence modelling tasks. Transformers are therefore more difficult to train images on. Pixels make up an image, and each image can include tens of thousands to millions of pixels. Each pixel will therefore perform a paired operation with each and every other pixel in the image in a transformer. An attention mechanism will expend $(500 \times 2) \times 2$ operations on an image with a dimension of 500×500 pixels. Even with many GPUs, this is a massive task. As a result, rather of using global attention when studying images, academics typically use some type of local attention (group of pixels). The

transformers are initially unsure of where each patch belongs. Positional embeddings thereby aid the transformer in determining where each patch belongs. The position of the patches was described using a straightforward numbering system of 1, 2, 3, etc. These are learnable vectors rather than only integers. That example, rather of using the number 1 directly, a lookup table that contains vectors for each number denoting the position of the patch is present. As a result, the first vector from the table is taken and placed in the transformer with the first patch. In a similar manner, for the second patch, the second vector from the table is taken and added to the transformer along with the second patch, and so on. This needs to be fed to the transformer in some fashion so that it can process it. Unrolling the image into a row/ column vector is one method of doing this. However, linear projection was utilized in [24]. This indicates that there is only one matrix, denoted by the letter E. The first step is to unroll a single patch into a linear vector. The embedding matrix E is then multiplied by this vector. The positional embedding and the final result are then sent to the transformer.

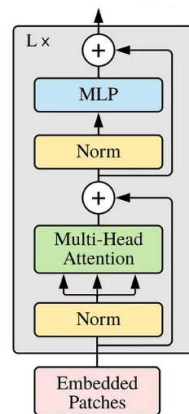


Fig. Architecture of Transformer Encoder [24]

A transformer encoder is then provided with all of the patches (linear projected) and each positional embedding. Standard transformer architecture is used in this transformer. The schematic view of the transformer based image classification approach is presented in the below Fig. XX

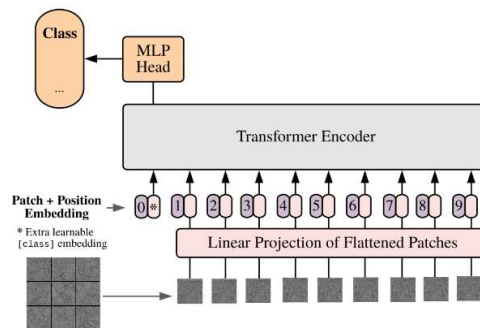


Fig. Schematic view of image classification with Transformer [24]

Performance Metrics

Accuracy does not account for class imbalance, it can be exceedingly deceptive. If the classifier merely predicts all negative samples correctly, it can still achieve above 90% accuracy when the positive to negative ratio is 10:100. Additionally, since machine learning algorithms make probabilistic assumptions about the data, we require a score that can account for the inherent

uncertainty involved in making predictions. One of the few metrics that can capture all of that is the Kappa score.

For multi-classification, Cohen's kappa coefficient (k) is a statistic that is used to assess inter-class similarity as well as intra-class similarity. Since it considers the potential that the similarity could have happened by chance, it is typically believed to be a more reliable measurement than a simple % agreement estimate.

$$k = \frac{p_o - p_e}{1 - p_e}$$

where p_o is the probability of similarity between predicted and ground truth labels; and p_e represents the probability that predicted and ground truth becomes similar by chance. The F1-Score is a measurement that combines recall and precision. Generally speaking, it is referred to as the harmonic mean of the two. Another method of determining a "average" of values is the harmonic mean, which is typically seen as better suited for ratios than the conventional arithmetic mean.

RESULTS AND DISCUSSION

The dataset considered for the experiments and analysis is slightly imbalanced and hence the focal loss is used as suggested in [25]. The Adam optimization algorithm was used in combination with weight decay mechanism. Weight loss in SGD and Adam is equivalently effective. For SGD, weight decay is the same as L2 regularization, but not for Adam. Weight decay and L2 regularization are not the same for Adam optimization algorithm. By re-parameterizing the weight decay factor dependent on the learning rate, the two strategies can be rendered equivalent for SGD; but, as is sometimes overlooked, this is not the case for Adam. L2 regularization, in particular, causes weights with large historic parameter and/or gradient amplitudes to be regularized less than they would be if utilizing weight decay when combined with adaptive gradients. The weight decay is implemented based on the following mathematical expression;

$\theta_{t+1} = (1 - \lambda)\theta_t - \alpha \nabla f_t(\theta_t)$ where λ represents the weight decay rate per training step; $\nabla f_t(\theta_t)$ denotes the t^{th} batch gradient and learning rate α . The value of different hyperparameters used in the model training process is given in the Table. XX. To increase the number of training images, data augmentation approaches were adopted.

Table. Hyperparameter values

Hyperparameter	Value
Weight Decay	0.0001
Learning Rate	0.001
Batch size	16
Epochs	50
# of neurons MLP block	64
Attention Dropout	0.2

Projection Dropout	0.2
# of transformer blocks	08

In the architecture of EANet, the self-attention layers used in the ViT are replaced with external attention. After a training of 50 epochs, the conventional transformer architecture which has 0.6M parameters based classification exhibited an accuracy level of ~89% test top-5 accuracy and ~64% top-1 accuracy. With same set of hyperparameters used in the experiments and same set of training samples, the EANet architecture which has 0.3M trainable parameters, showed higher accuracy of ~98% test top-5 accuracy and ~77% top-1 accuracy. This shall prove the effectiveness of external attention.

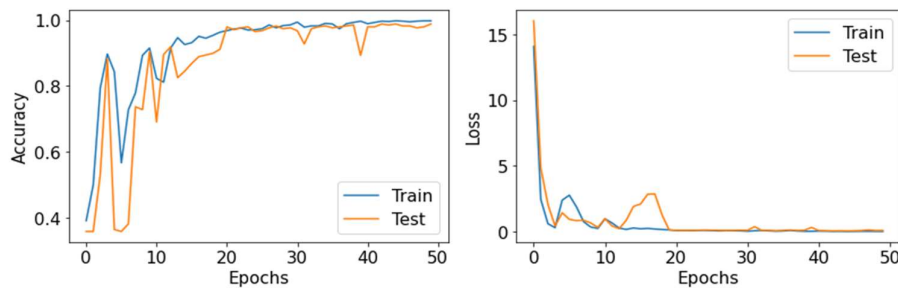


Fig. Performance analysis of EANet Architecture

The table given below summarizes the results of the experiments and the base line model (EANet) considered in this study. For effective investigation the kappa co-efficient is estimated for all the models. The results proved that the EANet composed of external attention mechanism with transformer technique exhibited better performance when compared to the other models in terms of precision, recall, and F1-Score. The pre-trained convolutional neural network performs poor when compared to the CNN+attention and EANet models. The class imbalance issue was handled by following the focal loss in combination with multi-class classification.

Table. Comparison of EANet performance with other models

Model	F1 Score	Accuracy	Kappa Co-Efficient
EANet	0.895	98.6	0.92
VGG + Attention	0.845	94.5	0.89
VGG	0.813	91.2	0.85

CONCLUSION

Transformer based approach has performed well in classifying the microscopic images of steel alloys. The images are divided in to patches and sent to the transformer encoder block. The attention layer aids the model in extracting therelevant features from even the lowest layer across the entire image. The MLP (multi-layer perceptron) layer performs the classification task and predicts 1 out of K classes after processing the encoded input. The performance of the

image classification transformer model was improved; further research can be conducted to enhance the self-supervised training approach. A transformer-based method for fault segmentation in metal surfaces could also be developed as future research in the line of seq to seq transformer model. Additional scalability of the transformer-based strategy might result in reduced computational time and better performance.

REFERENCES

1. W. D. Callister Jr, D. G. Rethwisch, *Fundamentals of Materials Science and Engineering: An Integrated Approach*, John Wiley & Sons, Hoboken; New Jersey 2020.
2. K. T. Butler, D. W. Davies, H. Cartwright, O. Isayev, A. Walsh, *Nature* 2018, **559**, 547.
3. S. Matsumoto, S. Ishida, M. Araki, T. Kato, K. Terayama, Y. Okuno, *Nat. Mach. Intell.* 2021, **3**, 153.
4. J. Hu, L. Shen, S. Albanie, G. Sun, and E. Wu, "Squeeze-and-excitation networks," *IEEE Trans. Pattern Anal. Mach. Intell.*, vol. 42, no. 8, pp. 2011–2023, 2020.
5. Guo, Meng-Hao, et al. "Beyond self-attention: External attention using two linear layers for visual tasks." *IEEE Transactions on Pattern Analysis and Machine Intelligence* (2022).
6. Dosovitskiy, Alexey, et al. "An image is worth 16x16 words: Transformers for image recognition at scale." *arXiv preprint arXiv:2010.11929* (2020).
7. M. Guo, J. Cai, Z. Liu, T. Mu, R. R. Martin, and S. Hu, "PCT: point cloud transformer," *Comput. Vis. Media*, vol. 7, no. 2, pp. 187–199, 2021.
8. S. Vosoughi, P. Vijayaraghavan, D. Roy, Tweet2Vec: learning tweet embeddings using character-level CNN-LSTM encoder-decoder, in: Proc. 39th Int. ACM SIGIR Conf. Res. Dev. Inf. Retr, Association for Computing Machinery, 18 M. Ge et al. / *Materials Today Nano* 11 (2020) 100087 New York, NY, USA, 2016, pp. 1041e1044
9. P.-S. Huang, X. He, J. Gao, L. Deng, A. Acero, L. Heck, Learning deep structured semantic models for web search using clickthrough data, in: Proc. 22nd ACM Int. Conf. Inf. Knowl. Manag, Association for Computing Machinery, New York, NY, USA, 2013, pp. 2333e2338
10. A. Graves, A. Mohamed, G. Hinton, Speech recognition with deep recurrent neural networks, in: 2013 IEEE Int. Conf. Acoust. Speech Signal Process, IEEE, 2013, pp. 6645e6649.
11. Z. Zhao, B. Zhao, F. Su, Person re-identification via integrating patch-based metric learning and local saliency learning, *Pattern Recogn.* 75 (2018) 90e98,
12. Y. Wu, M. Schuster, Z. Chen, Q.V. Le, M. Norouzi, W. Macherey, M. Krikun, Y. Cao, Q. Gao, K. Macherey, others, Google's Neural Machine Translation System: Bridging the Gap between Human and Machine Translation, *ArXivPrepr.*, 2016. ArXiv160908144
13. A. Agrawal, A. Choudhary, Deep materials informatics: applications of deep learning in materials science, *MRS Commun.* (2019) 1e14.
14. K. Ryan, J. Lengyel, M. Shatruk, Crystal structure prediction via deep learning, *J. Am. Chem. Soc.* 140 (2018) 10158e10168

15. D. Jha, L. Ward, A. Paul, W. Liao, A. Choudhary, C. Wolverton, A. Agrawal, Elemnet: deep learning the chemistry of materials from only elemental composition, *Sci. Rep.* 8 (2018) 17593.
16. W. Ye, C. Chen, Z. Wang, I.-H. Chu, S.P. Ong, Deep neural networks for accurate predictions of crystal stability, *Nat. Commun.* 9 (2018) 3800
17. R. Liu, A. Agrawal, W. Liao, A. Choudhary, M. De Graef, Materials discovery: understanding polycrystals from large-scale electron patterns, in: 2016 IEEE Int. Conf. Big Data Big Data, IEEE, 2016, pp. 2261e2269
18. B.L. DeCost, B. Lei, T. Francis, E.A. Holm, High throughput quantitative metallography for complex microstructures using deep learning: a case study in ultrahigh carbon steel, *Microsc. Microanal.* 25 (2019) 21-29.
19. K. de Haan, Z.S. Ballard, Y. Rivenson, Y. Wu, A. Ozcan, Resolution Enhancement in Scanning Electron Microscopy Using Deep Learning, *ArXivPrepr.*, 2019. ArXiv190111094.
20. M.H. Modarres, R. Aversa, S. Cozzini, R. Ciancio, A. Leto, G.P. Brandino, Neural network for nanoscience scanning electron microscope image recognition, *Sci. Rep.* 7 (2017) 13282.
21. C. Szegedy, V. Vanhoucke, S. Ioffe, J. Shlens, Z. Wojna, Rethinking the inception architecture for computer vision, in: *Proc. IEEE Conf. Comput. Vis. Pattern Recognit*, 2016, pp. 2818-2826
22. S.M. Azimi, D. Britz, M. Engstler, M. Fritz, F. Mücklich, Advanced steel microstructural classification by deep learning methods, *Sci. Rep.* 8 (2018) 2128.
23. M. Ziatdinov, A. Maksov, S.V. Kalinin, Learning surface molecular structures via machine vision, *NpjComput. Mater.* 3 (2017) 31
24. K. Jyothi Prakash. "Internet of things: IETF protocols, algorithms and applications." *Int. J. Innov. Technol. Explor. Eng.* 8.11 (2019): 2853-2857.
25. Sangamithra, B. "A memetic algorithm for multi objective vehicle routing problem with time windows." 2017 IEEE International Conference on Electrical, Instrumentation and Communication Engineering (ICEICE). IEEE, 2017.
26. Harika, A., et al. "Business process reengineering: issues and challenges." *Proceedings of Second International Conference on Smart Energy and Communication*. Springer, Singapore, 2021.
27. P. Sai Kiran,. "Resource aware virtual machine placement in IaaS cloud using bio-inspired firefly algorithm." *Journal of Green Engineering* 10 (2020): 9315-9327.
28. Natarajan, V. Anantha, et al. "Prediction Of Soil Ph From Remote Sensing Data Using Gradient Boosted Regression Analysis." *Journal of Pharmaceutical Negative Results* (2022): 29-36.
29. Kumar, M. Sunil, et al. "Automated Extraction of Non-Functional Requirements From Text Files: A Supervised Learning Approach." *Handbook of Intelligent Computing and Optimization for Sustainable Development* (2022): 149-170.
30. A. Dosovitskiy, L. Beyer, A. Kolesnikov, D. Weissenborn, X. Zhai, T. Unterthiner, M. Dehghani, M. Minderer, G. Heigold, S. Gelly, J. Uszkoreit, and N. Houlsby, "An image is worth 16x16 words: Transformers for image recognition at scale," in *ICLR*, 2021.

31. AnanthaNatarajan, V. "Forecasting of Wind Power using LSTM Recurrent Neural Network." *Journal of Green Engineering* 10 (2020).
32. Prasad, Tvs Gowtham, et al. "Cnn Based Pathway Control To Prevent Covid Spread Using Face Mask And Body Temperature Detection." *Journal of Pharmaceutical Negative Results* (2022): 1374-1381.
33. Burada, Sreedhar. "Computer-Aided Diagnosis Mechanism for Melanoma Skin Cancer Detection Using Radial Basis Function Network." *Proceedings of the International Conference on Cognitive and Intelligent Computing*. Springer, Singapore, 2022.
34. Kumar, M. Sunil, et al. "APPLYING THE MODULAR ENCRYPTION STANDARD TO MOBILE CLOUD COMPUTING TO IMPROVE THE SAFETY OF HEALTH DATA." *Journal of Pharmaceutical Negative Results* (2022): 1911-1917.
35. B. E. Manjunath Swamy. "Personalized Ranking Mechanism Using Yandex Dataset on Machine Learning Approaches." *Proceedings of the International Conference on Cognitive and Intelligent Computing*. Springer, Singapore, 2022.
36. Ganesh, D., et al. "Improving Security in Edge Computing by using Cognitive Trust Management Model." *2022 International Conference on Edge Computing and Applications (ICECAA)*. IEEE, 2022.
37. AnanthaNatarajan, V., Kumar, M. S., & Tamizhazhagan, V. (2020). Forecasting of Wind Power using LSTM Recurrent Neural Network. *Journal of Green Engineering*, 10.
38. Lin, T.Y., Goyal, P., Girshick, R., He, K., Dollar, P.: Focal loss for dense object detection. In: *2017 IEEE International Conference on Computer Vision (ICCV)*. pp. 2999–3007. IEEE (2017)